Salinity-Induced Calcium Signaling and Root Adaptation in Arabidopsis Require the Calcium Regulatory Protein Annexin1[1][W][OPEN]

Anuphon Laohavisit[2], Siân L. Richards, Lana Shabala, Chen Chen, Renato D.D.R. Colaço, Stéphanie M. Swarbreck, Emma Shaw[3], Adeeba Dark, Sergey Shabala, Zhonglin Shang, and Julia M. Davies*

Department of Plant Sciences, University of Cambridge, Cambridge CB2 3EA, United Kingdom (A.L., S.L.R., R.D.D.R.C., S.M.S., E.S., A.D., J.M.D.); School of Agricultural Sciences, University of Tasmania, Private Bag 54, Hobart, Tasmania 7001, Australia (L.S., S.S.); and College of Life Sciences, Hebei Normal University, Yuhua East Road, Shijiazhang, Hebei 050016, China (C.C., Z.S.)

Salinity (NaCl) stress impairs plant growth and inflicts severe crop losses. In roots, increasing extracellular NaCl causes Ca^{2+} influx to elevate cytosolic free Ca^{2+} ($[Ca^{2+}]_{cyt}$) as a second messenger for adaptive signaling. Amplification of the signal involves plasma membrane reduced nicotinamide adenine dinucleotide phosphate oxidase activation, with the resultant reactive oxygen species triggering Ca^{2+} influx. The genetic identities of the Ca^{2+}-permeable channels involved in generating the $[Ca^{2+}]_{cyt}$ signal are unknown. Potential candidates in the model plant Arabidopsis (*Arabidopsis thaliana*) include annexin1 (AtANN1). Here, luminescent detection of $[Ca^{2+}]_{cyt}$ showed that AtANN1 responds to high extracellular NaCl by mediating reactive oxygen species-activated Ca^{2+} influx across the plasma membrane of root epidermal protoplasts. Electrophysiological analysis revealed that root epidermal plasma membrane Ca^{2+} influx currents activated by NaCl are absent from the *Atann1* loss-of-function mutant. Both adaptive signaling and salt-responsive production of secondary roots are impaired in the loss-of-function mutant, thus identifying AtANN1 as a key component of root cell adaptation to salinity.

Soil salinity is an increasing threat to global crop productivity, with up to one-third of agricultural land affected (Munns and Tester, 2008; Kronzucker and Britto, 2011). Salinity (NaCl) stress impairs plant growth and inflicts severe crop losses (Munns and Tester, 2008). Raised concentrations in soil solution or irrigation water perturb osmotic relations, making it difficult for roots to take up water. Uptake of Na^+ deleteriously affects the cellular K^+:Na^+ ratio and may lead to cell death. In roots, high extracellular NaCl causes Ca^{2+} influx to elevate cytosolic free Ca^{2+} ($[Ca^{2+}]_{cyt}$) as a second messenger for adaptive signaling (Lynch et al., 1989; Kiegle et al., 2000; Shi et al., 2000; Tracy et al., 2008). Exposure to salinity activates the Salt Overly Sensitive (SOS) pathway, leading to Ca^{2+}-dependent increased activity of SOS1, a plasma membrane Na^+-H^+ antiporter that enables adaptation through Na^+ efflux (Shi et al., 2000; Chung et al., 2008). Salinity also increases *SOS1* expression in Arabidopsis (*Arabidopsis thaliana*), and this requires activation of the AtSOS3/calcineurin B-like4 Ca^{2+} sensor (Shi et al., 2000). Reactive oxygen species (ROS), sourced from plasma membrane NADPH oxidase activity, help stabilize *AtSOS1* transcripts (Chung et al., 2008). Growth of better-adapted secondary roots is impaired in *Atsos1* (Huh et al., 2002) and involves superoxide anion production, possibly by NADPH oxidases (Roach and Kranner, 2011). These enzymes are now known to play a role in xylem loading of Na^+ (Jiang et al., 2012).

The channels involved in transiently elevating $[Ca^{2+}]_{cyt}$ in response to increasing extracellular NaCl have not been identified at the genetic level. Manipulation of membrane voltage by varying external concentrations of K^+ and Ca^{2+} has indicated that both hyperpolarization- and depolarization-activated plasma membrane Ca^{2+}-permeable channels can operate in generating a NaCl-induced $[Ca^{2+}]_{cyt}$ increase (Tracy et al., 2008). The Arabidopsis genome contains two families of channel subunit genes that may contribute to NaCl-induced signaling, the Cyclic Nucleotide-Gated Channels (CNGC) and the Glu Receptors (Dodd et al., 2010) Members of both groups have been shown to be

[1] This work was supported by the Biotechnology and Biological Sciences Research Council, the Royal Society, European Union FP7 Marie Curie Actions, the Australian Research Council, and the Grain Research and Development Corporation.

[2] Present address: Riken Plant Science Center, 1–7–22 Suehiro-cho, Tsurumi-ku, Yokohama City, Kanagawa 230–0045, Japan.

[3] Present address: Forum for the Future, Overseas House, 19–23 Ironmonger Row, London EC1V 3QN, UK.

* Address correspondence to jmd32@cam.ac.uk.

The author responsible for distribution of materials integral to the findings presented in this article in accordance with the policy described in the Instructions for Authors (www.plantphysiol.org) is: Julia Davies (jmd32@cam.ac.uk).

[W] The online version of this article contains Web-only data.

[OPEN] Articles can be viewed online without a subscription.

www.plantphysiol.org/cgi/doi/10.1104/pp.113.217810

competent in plasma membrane Ca^{2+} flux (Ali et al., 2007; Vincill et al., 2012), but none have been shown to function in NaCl-induced $[Ca^{2+}]_{cyt}$ elevation.

Plant annexins have been shown to form Ca^{2+}-permeable channels in planar lipid bilayers (Laohavisit et al., 2009, 2010, 2012). These soluble proteins are capable of membrane binding and insertion (for review, see Laohavisit and Davies, 2011). The most abundant annexin in Arabidopsis, AtANN1, can exist as a plasma membrane protein (Lee et al., 2004) and is responsible for the root epidermal plasma membrane Ca^{2+}- and K^+-permeable conductance that is activated by extracellular hydroxyl radicals ($OH^•$), the most reactive of the ROS (Laohavisit et al., 2012). In this study, we have tested for the involvement of AtANN1 in the generation of root and root epidermal NaCl-induced $[Ca^{2+}]_{cyt}$ elevation. In most cases, high concentrations of NaCl were tested, as these are known to promote extracellular $OH^•$ formation (Demidchik et al., 2010), cause accumulation of AtANN1 in membranes (Lee et al., 2004), and promote secondary root formation (Huh et al., 2002). Results show that AtANN1 does not contribute to root Na^+ uptake but is a component of the $[Ca^{2+}]_{cyt}$ signal, particularly that generated at the extracellular $[Ca^{2+}]$ of saline soils and by production of ROS. The impairment in $[Ca^{2+}]_{cyt}$ signaling is reflected in the poor ability of *Atann1* roots to up-regulate NaCl-responsive transcripts and generate secondary roots when grown in saline conditions.

RESULTS

AtANN1 Restricts Root Epidermal Net Na^+ Influx and Mediates NaCl-Induced $[Ca^{2+}]_{cyt}$ Elevation

Na^+ entry into root cells is mediated by plasma membrane nonselective cation channels (Demidchik and Tester, 2002; Gobert et al., 2006; Guo et al., 2008; Kronzucker and Britto, 2011). As AtANN1 was found previously to have plasma membrane cation transport activity (Laohavisit et al., 2012), we first tested for AtANN1's possible participation in Na^+ entry by measuring net fluxes at root epidermal cells using a vibrating ion-selective microelectrode (Shabala et al., 2006). Wild-type cells sustained a maximum mean net Na^+ influx of 2,023 ± (SE) 732 nmol m^{-2} s^{-1} when challenged with 50 mM NaCl (1 mM extracellular Ca^{2+}), followed by a recovery phase (Fig. 1A; $n = 4$). Maximum mean net Na^+ influx for the *Atann1* loss-of-function mutant (Lee et al., 2004; Laohavisit et al., 2012) was significantly higher than the wild type (12,538 ± 3,032 nmol m^{-2} s^{-1}, $P = 0.02$, Student's t test; $n = 5$; Fig. 1A).

High extracellular salinity increases net K^+ efflux from roots (Shabala et al., 2006). Net K^+ efflux from *Atann1* ($n = 5$) was also significantly (2-fold) higher than the wild type ($n = 4$; $P = 0.04$; Fig. 1B), commensurate with the mutant's greater net Na^+ influx. Isoosmotic controls using D-sorbitol showed that responses were due to NaCl rather than osmotic stress ($n = 5$; Fig. 1, A and B). Resolving net Na^+ fluxes at higher NaCl concentrations was not possible due to methodological limitations, but increasing NaCl stress to 220 mM also caused significantly greater net K^+ release from *Atann1* compared with the wild type (wild-type peak efflux, –737 ± 108 nmol m^{-2} s^{-1}, $n = 4$; *Atann1*, –1,270 ± 22 m^{-2} s^{-1}, $n = 7$; $P = 0.003$). These results show that AtANN1 is effectively a negative regulator of net Na^+ influx. As AtANN1 is a plasma membrane cation channel that can mediate K^+ efflux (Gorecka et al., 2007; Laohavisit et al., 2012), we anticipated that *Atann1* should have lower Na^+-induced K^+ loss than the wild type. That K^+ efflux was greater in the mutant was not consistent with simply a loss of K^+ efflux function.

We reasoned that greater epidermal Na^+ influx could elicit a larger $[Ca^{2+}]_{cyt}$ signal in *Atann1* than the wild

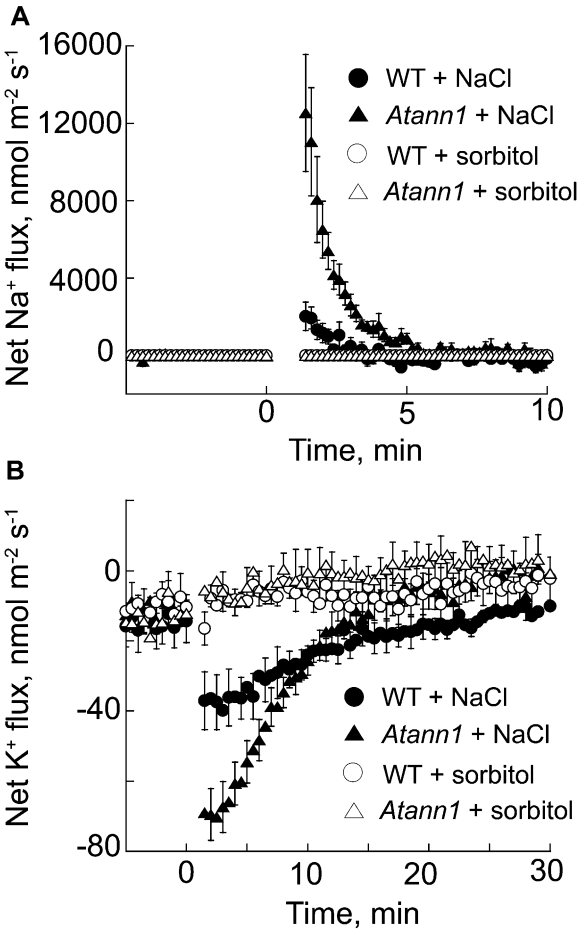

Figure 1. NaCl causes greater net Na^+ influx and K^+ efflux at root epidermal cells of *Atann1* than of the wild type (WT). Net fluxes in response to 50 mM NaCl were measured using a vibrating ion-selective microelectrode; bathing solution was 1 mM $CaCl_2$, 0.1 mM KCl, and 2 mM MES/Tris, pH 6. Measurements in the first 60 s after test addition were discarded to allow for establishment of diffusion gradients. The sign convention is "influx positive." A, Mean ± SE net Na^+ fluxes of the wild type (circle) and *Atann1* (triangle) in response to addition of NaCl (black symbol) or the D-sorbitol osmotic equivalent (white symbol) as indicated by the arrow ($n = 4$–7 roots). B, Net K^+ fluxes in response to NaCl or the D-sorbitol osmotic equivalent ($n = 4$–7 roots).

type. To investigate this, root epidermal protoplasts were isolated from plants cytosolically expressing aequorin as a $[Ca^{2+}]_{cyt}$ indicator (Laohavisit et al., 2012). With extracellular Ca^{2+} at 1 mM (as in flux experiments), NaCl (220 mM) evoked a rapid, monophasic, and transient $[Ca^{2+}]_{cyt}$ increase (Fig. 2A) that was significantly lower in *Atann1* than the wild type, both in terms of initial increment ($P = 0.023$; $n = 4$ for *Atann1* and 8 for the wild type) and total $[Ca^{2+}]_{cyt}$ mobilized ($P = 0.025$); no significant differences between genotypes were observed for the osmotic control (Fig. 2B; initial increment, $P = 0.30$; total $[Ca^{2+}]_{cyt}$ mobilized, $P = 0.185$, $n = 4$ for *Atann1* and 8 for the wild type). There was no significant difference between NaCl- and osmotically induced $[Ca^{2+}]_{cyt}$ elevation by the wild type, but these data show that AtANN1 is required for a significant NaCl-specific increase in $[Ca^{2+}]_{cyt}$ at 1 mM Ca^{2+}.

AtANN1 Mediates NaCl-Induced Ca^{2+} Influx at the High Extracellular Ca^{2+} Found in Saline Soils

Extracellular Ca^{2+} was increased to 10 mM to mimic saline soils (Kronzucker and Britto, 2011). Under these conditions, there were no statistically significant differences in the "touch" control responses between the wild type and *Atann1* (Supplemental Fig. S1A). Elevation of extracellular Ca^{2+} to 10 mM significantly increased the total $[Ca^{2+}]_{cyt}$ mobilized by wild-type root epidermal protoplasts in response to 220 mM NaCl (Fig. 2C; $P = 0.001$, $n = 8$), and the response was not significantly different from the osmotic control. Elevations of $[Ca^{2+}]_{cyt}$ in the wild type were significantly inhibited by the Ca^{2+} channel blocker Gd^{3+}, which also blocks AtANN1 channel activity (Laohavisit et al., 2012), demonstrating reliance on Ca^{2+} influx (Supplemental Fig. S1B; total $[Ca^{2+}]_{cyt}$ mobilized, $P = 0.0003$, $n = 3$). In the same test on the *Atann1* mutant, an irregular $[Ca^{2+}]_{cyt}$ response to NaCl was observed, indicating residual Gd^{3+}-sensitive and -insensitive components, but overall no significant differences were found (Supplemental Fig. S1C; $n = 3$). *Atann1* protoplasts were unresponsive to increased extracellular Ca^{2+} under both NaCl (Fig. 2D; $P = 0.86$, $n = 8$) and isoosmotic challenge (Supplemental Fig. S1D; total $[Ca^{2+}]_{cyt}$ mobilized, $P = 0.877$; although kinetics appear altered, there was no significant difference in time taken to reach peak response, $P = 0.87$; $n = 8$). The $[Ca^{2+}]_{cyt}$ responses to 150 mM NaCl were also significantly lower in *Atann1* compared with the wild type at 10 mM extracellular Ca^{2+} (Supplemental Fig. S1E; initial $[Ca^{2+}]_{cyt}$ increment, $P = 0.038$; total $[Ca^{2+}]_{cyt}$ mobilized, $P = 0.001$, $n = 6$). At whole-root level (Supplemental Fig. S2, A–D), there were no statistically significant differences in total $[Ca^{2+}]_{cyt}$ increase between *Atann1* and the wild type challenged with 50 to 250 mM NaCl or its osmotic equivalent (Supplemental Fig. S2E; $n = 3$). This is perhaps to be expected, given

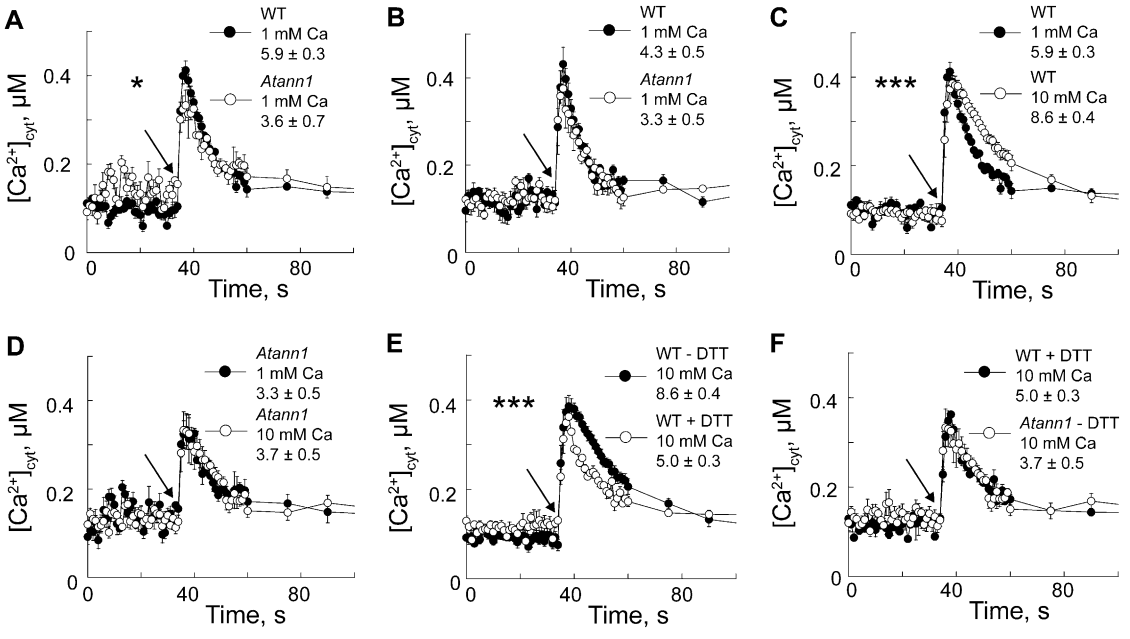

Figure 2. $[Ca^{2+}]_{cyt}$ signaling is impaired in *Atann1* root epidermal protoplasts. A, Mean ± SE $[Ca^{2+}]_{cyt}$ response of wild-type (WT; black circle) and *Atann1* (white circle) protoplasts (70 per µL; 0.1 mM KCl and 2 mM Tris/MES, pH 5.8) in response to 220 mM NaCl added at 35 s indicated by arrow) with 1 mM extracellular Ca^{2+} ($n = 4$; inset, mean ± SE total $[Ca^{2+}]_{cyt}$ mobilized). B, Same as A but with isotonic D-sorbitol ($n = 4$). C, Increasing extracellular Ca^{2+} from 1 mM (black circle) to 10 mM (white circle) increased wild-type response to 220 mM NaCl ($n = 8$). D, *Atann1* response to 220 mM NaCl with 10 mM Ca^{2+} (black circle) did not differ from that with 1 mM Ca^{2+} (white circle; $n = 4$). E, At 10 mM Ca^{2+}, DTT (1 mM; black circle) lowers wild-type $[Ca^{2+}]_{cyt}$ response to 220 mM NaCl ($n = 4$). F, At 10 mM Ca^{2+}, *Atann1* (white circle) without DTT phenocopies the wild-type response to 220 mM NaCl with DTT (black circle; $n = 8$). Asterisk denotes level of significance difference.

that cell-specific changes in $[Ca^{2+}]_{cyt}$ measured with aequorin may not manifest at the whole-organ level (Dodd et al., 2006; Laohavisit et al., 2012). At the highest [NaCl], secondary peak increases in $[Ca^{2+}]_{cyt}$ were more pronounced in *Atann1* than in the wild type (Supplemental Fig. S2, A and C), suggesting a role for AtANN1 in regulating the response.

AtANN1 Is Required for ROS-Induced $[Ca^{2+}]_{cyt}$ Elevation on NaCl Exposure

On exposure to extracellular NaCl, plasma membrane NADPH oxidases are activated to produce extracellular superoxide anion (Yang et al., 2007; Chung et al., 2008; Kaye et al., 2011; Xie et al., 2011; Jiang et al., 2012; Liu et al., 2012; Ma et al., 2012). This drives production of extracellular $OH^{\bullet}$, with up to a 5-fold increase in $[OH^{\bullet}]$ detected in NaCl-stressed Arabidopsis roots (Demidchik et al., 2010). AtANN1 forms the root epidermal plasma membrane Ca^{2+}-permeable channel conductance that is activated by extracellular $OH^{\bullet}$ (Laohavisit et al., 2012), suggesting that it could contribute to the plasma membrane Ca^{2+} influx pathway acting downstream of NADPH oxidase activity in salt stress (Chung et al., 2008; Ma et al., 2012). Reducing conditions were imposed (with 1 mM dithiothreitol [DTT]) on wild-type root epidermal protoplasts (expressing aequorin) to oppose ROS activation of plasma membrane Ca^{2+} channels (Demidchik et al., 2009) in response to NaCl. There was no significant effect of DTT on touch responses (Supplemental Fig. S1; $n = 4$). The initial $[Ca^{2+}]_{cyt}$ increase of wild-type protoplasts in response to 220 mM NaCl (in 10 mM Ca^{2+}) was not significantly lowered by reducing conditions (Fig. 2E; $P = 0.26$), but the total $[Ca^{2+}]_{cyt}$ mobilized was significantly lowered ($P = 0.0001$, $n = 4$ for + DTT, $n = 8$ for – DTT), consistent with NaCl stress activating a later and ROS-dependent $[Ca^{2+}]_{cyt}$ response. *Atann1* without DTT ($n = 8$) phenocopied the wild type's response to NaCl with DTT ($n = 4$; Fig. 1F; no significant difference), clearly showing that AtANN1 was responsible for the ROS-dependent (i.e. DTT-inhibited) component of the $[Ca^{2+}]_{cyt}$ response.

We tested the ability of AtANN1 to function in this process by assaying for Ca^{2+}, K^+, and Na^+ permeability of the $OH^{\bullet}$-activated AtANN1 ionic conductance. Recombinant AtANN1 was incorporated from the equivalent of the cytosol (cis compartment) into artificial planar lipid bilayers as mimetics of the plant plasma membrane. Na^+ and Ca^{2+} gradients across the bilayer qualitatively simulated in vivo gradients under salinity stress and activation by $OH^{\bullet}$ (at the equivalent of the extracellular face of the plasma membrane, trans compartment) was achieved by addition of 1 mM Cu^{2+} and 1 mM ascorbate, as described previously (Laohavisit et al., 2012). An $OH^{\bullet}$-activated current was evident that was blocked by 50 μM Gd^{3+} at the trans face, indicating that AtANN1 mediated the current across the bilayer (Fig. 3A; Supplemental Fig. S3). Boiled AtANN1 did not

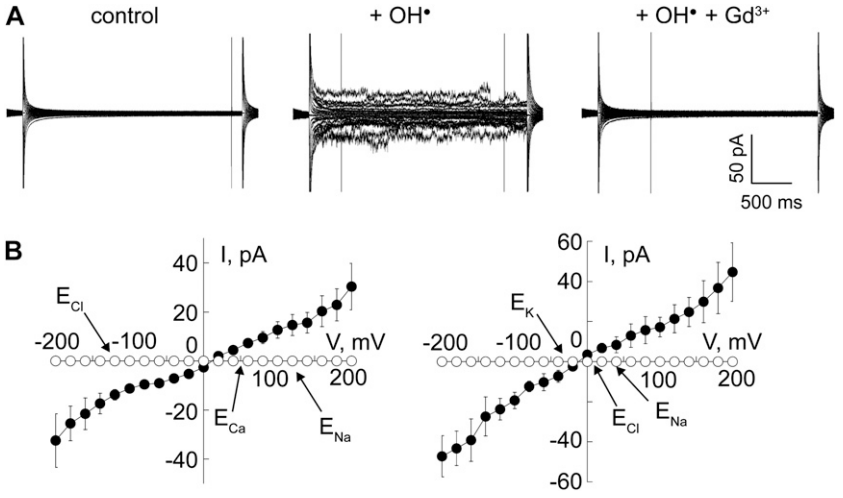

Figure 3. Recombinant AtANN1 forms an $OH^{\bullet}$-activated Ca^{2+}-permeable conductance that is weakly permeable to Na^+. AtANN1 (3 μg) was incorporated from the cis chamber into a planar lipid bilayer and exposed to $OH^{\bullet}$ generated at the opposite (trans) membrane face. A, Macroscopic currents recorded from a representative trial in response to voltage steps of 20-mV increments from –200 to +200 mV, applied from a 0-mV baseline with cis 200 mM $CaCl_2$ and 200 mM NaCl (pH 6), and trans 1 mM $CaCl_2$ and 1 mM NaCl (pH 6). The pH was set with 10 mM Tris/Bis-Tris propane. Left, control; middle, maximum current in response to trans $OH^{\bullet}$; and right, with trans $OH^{\bullet}$ and Gd^{3+}. Magnified traces of control and $OH^{\bullet}$-activated currents are shown in Supplemental Figure S3. B, Mean ± SE current-voltage relationships from six individual trials using conditions described in A; $OH^{\bullet}$-activated conductance (black circles) and $OH^{\bullet}$-activated conductance blocked by Gd^{3+} (white circles). Equilibrium potentials (E) are marked by arrows. Current flowing below the *v* axis is cation flow from trans to cis or anion flow from cis to trans. C, Mean ± SE current-voltage relationships of the $OH^{\bullet}$-activated conductance (black circles) with cis 200 mM KCl and 50 mM NaCl (pH 6) and trans 50 mM KCl and 200 mM NaCl (pH 6); mean ± SE E_{rev} was –10.7 ± 2.4 mV ($n = 4$).

generate a conductance (Supplemental Fig. S3; $n = 3$). The AtANN1-mediated $OH^{\bullet}$-activated conductance was Ca^{2+} permeable, with the reversal voltage ($[E_{rev}]$, at which net current is 0; +10 ± 6 mV; $n = 6$) lying close to the equilibrium potential for Ca^{2+} rather than Na^{+} (Fig. 3B). E_{rev} of the AtANN1-mediated currents were used to estimate permeabilities. A Na^{+}-to-Cl^{-} permeability ratio of 3 was estimated (Supplemental Fig. S3; $n = 6$). The Ca^{2+}-to-Na^{+} permeability ratio was 11 ($n = 6$; Fig. 3B), two orders of magnitude higher than the previously determined Ca^{2+}-to-K^{+} permeability ratio of 0.64 under identical recording conditions (Laohavisit et al., 2012), thus showing that AtANN1 would be competent to amplify the $[Ca^{2+}]_{cyt}$ signal while resisting further Na^{+} ingress. Na^{+} permeated poorly relative to K^{+} with a permeability ratio of 18 (Fig. 3C; $n = 6$).

AtANN1 Is Required for NaCl-Induced Ca^{2+} Influx Currents across Root Epidermal Plasma Membrane

Patch clamp electrophysiology experiments on wild-type Arabidopsis root protoplasts have shown that 50 mM NaCl causes a plasma membrane hyperpolarization-activated Ca^{2+} influx current to form after 15 min and that this relies on NADPH oxidase activity to generate ROS (Ma et al., 2012). Here, in patch clamp trials on root epidermal protoplasts (no aequorin), 50 mM NaCl evoked a significant increase in wild-type plasma membrane hyperpolarization-activated Ca^{2+} influx current after 20 min exposure (Fig. 4; $n = 6$; $P < 0.05$), while *Atann1* did not respond (Fig. 4; $n = 6$). The efflux currents evoked in the wild type at depolarized voltages (carrying Ca^{2+} and K^{+}) were also absent from *Atann1*. Both influx and efflux currents were restored by complementation of the *Atann1* mutant (Fig. 4; $n = 6$). The presence of DTT in the bath and pipette solutions prevented current activation by NaCl in the wild type (Fig. 4; $n = 6$), demonstrating the need for ROS production. This phenocopying of the *Atann1* mutant (without DTT) supports AtANN1's mediating a ROS-activated conductance. Higher concentrations of NaCl were not tested, as they destabilize the seal between the membrane and patch clamp electrode (Shabala et al., 2006). Overall, the aequorin and electrophysiology data show that oxidation shapes the $[Ca^{2+}]_{cyt}$ response to NaCl at high extracellular Ca^{2+}, with AtANN1 mediating an oxidation-activated Ca^{2+} influx component.

NaCl-Induced Transcription and Adaptive Root Growth Are Impaired in Atann1

Transcripts of the salinity and osmotic stress-responsive genes *Responsive to Dessication29A* (*AtRD29A*), *Dehydration-Responsive Element Binding2A* (*AtDREB2A*), and *AtDREB2B* (Dinneny et al., 2008; Nakashima et al., 2009; Kaye et al., 2011) were all significantly up-regulated in the wild type and *Atann1* roots at 24 h of NaCl exposure, with extracellular Ca^{2+} at 1.5 mM (Supplemental Fig. S4). Up-regulation of *AtRD29A* was significantly lower in

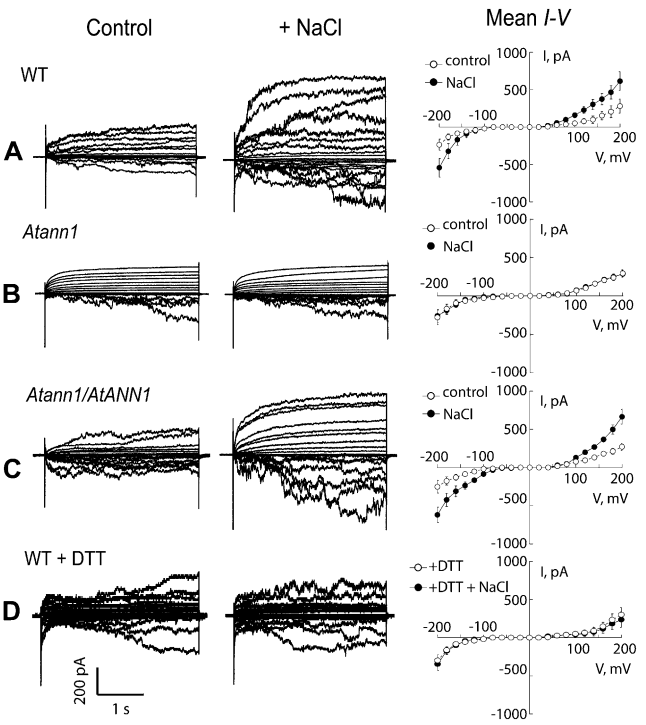

Figure 4. NaCl-activated root epidermal plasma membrane currents require AtANN1. Currents from A, the wild type; B, *Atann1*; C, *AtANN1/Atann1*; and D, the wild type with 1 mM DTT (in bath and pipette solutions) were sampled using the patch clamp "whole-cell" mode under control conditions (white circle) and after exposure to 50 mM NaCl (black circles). There were no significant differences in control currents between genotypes. Data are mean ± SE, and maximal NaCl-activated currents are shown ($n = 6$). Current flowing below the voltage axis is net positive charge entering the protoplast. Ca^{2+} influx occurs in the physiological voltage range. At voltages more negative than the equilibrium potential for K^{+} (–156 mV), K^{+} influx is a possible component of the inward current. Bathing solution for epidermal protoplasts comprised 20 mM $CaCl_2$, 0.1 mM KCl, 20 μM NaCl, and 5 mM MES-Tris, pH 5.6, adjusted to 270 mOsm with D-sorbitol. Pipette solution comprised 40 mM K-gluconate, 10 mM KCl, 0.4 mM $CaCl_2$, 1 mM bis(2-aminophenoxy)ethane-*N*,*N*,*N*′,*N*′-tetraacetic acid, and 2 mM MES-Tris, pH 7.2, adjusted to 270 mOsm with D-sorbitol.

Atann1 compared with the wild type (two-way ANOVA; $P = 0.05$; Supplemental Fig. S4). *AtSOS1* was up-regulated in wild-type roots to levels comparable with a previous study on chronic salinity stress (Dinneny et al., 2008) but was not up-regulated in *Atann1*, consistent with AtANN1's operation in $[Ca^{2+}]_{cyt}$-driven signaling (Fig. 5A; $P < 0.05$, $n = 3$). Impaired $[Ca^{2+}]_{cyt}$ signaling under salinity stress should be deleterious to adaptive root growth. Secondary root production under salinity stress at an extracellular $[Ca^{2+}]$ of 1.5 mM was significantly impaired in *Atann1*, confirming this annexin's involvement in adaptive root growth (Fig. 5, B and C; $n = 4$). When extracellular $[Ca^{2+}]$ was increased to 10 mM, wild-type secondary root production was not changed; it was still impaired in *Atann1*, but this was not significantly different to the wild type (300 mM

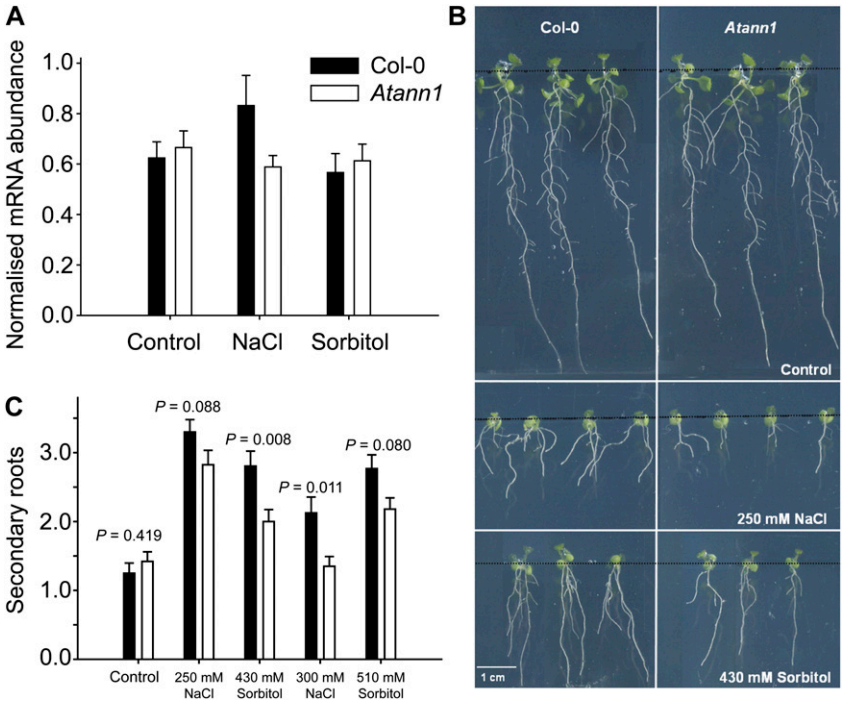

Figure 5. Root adaptation to salinity requires AtANN1. A, *AtSOS1* transcript abundance increases under chronic salinity exposure (150 mM NaCl, 24 h) of wild-type (black bar) but not *Atann1* (white bar) roots. The isoosmotic control was 275 mM sorbitol. Mean ± SE transcript abundance (assayed by quantitative PCR) from three trials with 40 roots per genotype and test. B, *Atann1* development of secondary roots in response to growth on 250 NaCl or isoosmotic sorbitol was impaired. Plants are shown 9 d after transfer to control or test plates. Black, horizontal lines demarcate the junction between control medium (top) and test (bottom). C, Mean ± SE secondary roots, 9 d after transfer to control or test plates. Data are from four trials using 36 to 40 plants per genotype per treatment with seed from two separate harvests. Black bar, the wild type and white bar, *Atann1*. Significance was tested with the Student's *t* test or Mann-Whitney U rank sum test, if data were not normally distributed.

NaCl, mean ± SE: wild type, 2 ± 0.7; *Atann1*, 1.6 ± 0.2, $n = 3$).

DISCUSSION

AtANN1 Restricts Na^+ Influx

Root epidermal cells are initial sensing points of soil conditions and are where root expression of *AtANN1* is highest (Dinneny et al., 2008). The low permeability of AtANN1 to Na^+ and the greater net epidermal Na^+ influx of the *Atann1* mutant suggest that this annexin does not contribute to Na^+ uptake. Rather, it suggests that AtANN1 is a negative regulator of Na^+ influx that may be influencing activity of Na^+ uptake routes such as AtCNGC3 and AtCNGC10 (Gobert et al., 2006; Guo et al., 2008), posttranslationally or even at transcriptional level. It was found previously that the mutant's root epidermal plasma membrane voltage was not significantly different to the wild type (Laohavisit et al., 2012), indicating that greater Na^+ influx is not simply the effect of a more negative voltage. The greater NaCl-induced K^+ efflux from the mutant could simply be the consequence of greater Na^+ influx but could be indicative of a greater driving force for K^+ efflux, given the loss of AtANN1 as a plasma membrane K^+ efflux pathway and hence potential accumulation of K^+ as a consequence. NaCl-induced K^+ efflux from roots is mediated in part by extracellular $OH^\bullet$ activating the plasma membrane K^+ channel Guard Cell Outwardly Rectifying K (GORK; Demidchik et al., 2010). GORK responds normally to extracellular $OH^\bullet$ in *Atann1* (Laohavisit et al., 2012) and should be functional in the studies here. AtANN1 has peroxidase activity (Konopka-Postupolska et al., 2009) and can be extracellular (Laohavisit and Davies, 2011). Therefore, the NaCl-stressed *Atann1* mutant may have greater capacity for extracellular $OH^\bullet$ production (resulting from increased hydrogen peroxide concentration), leading to greater GORK activation and K^+ efflux. However, AtANN1 peroxidase activity is very weak, and because it is a copper-binding protein that could catalyze $OH^\bullet$ production (Kung et al., 2006), its absence could just as readily lead to less GORK activation. The mechanisms underlying the perturbed Na^+ and K^+ fluxes now require elucidation.

AtANN1-Dependent Mobilization of Ca^{2+} Depends on Extracellular Ca^{2+} and ROS

The ionic component of NaCl stress might be expected to cause a greater $[Ca^{2+}]_{cyt}$ elevation than the hyperosmotic component, but intriguingly, there were no significant differences between the wild type's $[Ca^{2+}]_{cyt}$ elevation in response to NaCl and isoosmotic sorbitol. This does not, however, preclude subtle differences that could not be resolved by aequorin or differences in the mechanisms of $[Ca^{2+}]_{cyt}$ elevation. Results here show AtANN1's involvement in mobilizing Ca^{2+} under salinity exposure, with its effect on epidermal $[Ca^{2+}]_{cyt}$ dependent on the concentration of extracellular Ca^{2+} and the production of ROS. At 1 mM extracellular Ca^{2+}, AtANN1 contributes to the initial $[Ca^{2+}]_{cyt}$ increase and total $[Ca^{2+}]_{cyt}$ mobilized in response to a NaCl-specific component of the response to salinity. How AtANN1 works at this extracellular $[Ca^{2+}]$ now

needs to be determined. As Arabidopsis roots produce extracellular $OH^{\bullet}$ in response to NaCl even at 0.1 mM Ca^{2+} (Demidchik et al., 2010), it remains feasible that AtANN1 mediates $OH^{\bullet}$-activated Ca^{2+} influx at 1 mM extracellular Ca^{2+}. Clearly, other transport pathways are operating at the hyperpolarizing voltage favored by the low $[K^+]$ assay solution (representing typical soil solution K^+), and these now need to be identified.

In the presence of 220 mM NaCl, AtANN1 is required for the additional epidermal $[Ca^{2+}]_{cyt}$ increase caused by raising external Ca^{2+} to the 10 mM Ca^{2+} found in saline soils. With the degree of resolution afforded by aequorin, this does not appear to be NaCl specific but an osmotic response. At this external Ca^{2+} concentration, AtANN1 accounts for the ROS-sensitive component of salinity-induced $[Ca^{2+}]_{cyt}$ generation. This is consistent with our finding (using patch clamping) that AtANN1 is a necessary component of the epidermal plasma membrane Ca^{2+} influx conductance activated by NaCl and known from a previous study to require NADPH oxidase activity (Ma et al., 2012). We envisage that as NADPH oxidase activity and extracellular $OH^{\bullet}$ production by roots increase under high salinity stress (Yang et al., 2007; Demidchik et al., 2010; Kaye et al., 2011; Xie et al., 2011; Liu et al., 2012; Ma et al., 2012), AtANN1 fulfills its previously defined role of mediating the root epidermal plasma membrane Ca^{2+} influx conductance that is activated by extracellular $OH^{\bullet}$ (Laohavisit et al., 2012). The current-voltage relationship of recombinant AtANN1 in vitro suggests that AtANN1's contribution to Ca^{2+} influx across the plasma membrane would decline if membrane voltage depolarized, for example through increased soil $[K^+]$. Although the mechanism through which AtANN1 forms a transbilayer conductance is unclear, its ability shown in this study to form an $OH^{\bullet}$-activated Ca^{2+}-permeable conductance that can discriminate against Na^+ agrees well with a role in Ca^{2+} signaling during salinity stress.

AtANN1-Dependent Transcription and Root Growth

ROS levels in Arabidopsis roots are elevated for the first 24 h of exposure to NaCl (Xie et al., 2011), and we found significant up-regulation of salinity and osmotic stress-responsive genes at this time point. Salt stress induction of *AtRD29A* requires NADPH oxidase activity (Kaye et al., 2011), and the failure of the *Atann1* mutant to show normal induction (with NaCl but not the osmotic equivalent) agrees with a role for AtANN1 in mediating a NaCl-specific ROS-dependent component of Ca^{2+} signaling, at low (1.5 mM) external Ca^{2+}. A role for *AtRD29A* in production of secondary roots during salt stress has yet to be determined, but it is interesting that its transcription under osmotic stress was not significantly affected in *Atann1* (agreeing with protoplast $[Ca^{2+}]_{cyt}$ responses), but secondary root production was. This shows that AtANN1 can act in secondary root formation induced by the osmotic component of salinity stress at low external Ca^{2+} independently of epidermal $[Ca^{2+}]_{cyt}$ signaling. NaCl-induced secondary root production does involve AtSOS1 (Huh et al., 2002). Transcriptional up-regulation of *AtSOS1* in the wild type is known to be small (Dinneny et al., 2008). In wild-type roots (at 1.5 mM external Ca^{2+}), NaCl caused greater AtSOS1 up-regulation than the isoosmotic control, showing that the effect was specific to the ionic component of the treatment. This up-regulation failed in *Atann1* (at 1.5 mM external Ca^{2+}), and although a causal link between epidermal signaling and root growth cannot be made, this is in agreement with the loss of a NaCl-specific component of salinity-induced $[Ca^{2+}]_{cyt}$ elevation at low external Ca^{2+}. This lesion in At*SOS1* regulation may have contributed to the mutant's poor germination under saline conditions (Lee et al., 2004), and it is expected that cytosolic $[Na^+]$ content of *Atann1* would be higher than the wild type. Stability of the *AtSOS1* transcript specifically requires the Respiratory Burst Oxidase Homolog C (AtRBOHC) NAPDH oxidase and extracellular $OH^{\bullet}$ production (Chung et al., 2008). Although other NADPH oxidases, such as AtRBOHJ (Kaye et al., 2011), are involved in adaptation to salinity, there appears to be an absolute requirement for AtRBOHC in salt-induced AtSOS1 transcript stability (Chung et al., 2008). As AtANN1 mediates the extracellular $OH^{\bullet}$-activated Ca^{2+} influx pathway in the epidermis (Laohavisit et al., 2012) and it is likely that it relies on AtRBOHC for ROS generation (Foreman et al., 2003), we postulate that AtANN1 lies downstream of AtRBOHC in stabilization of *AtSOS1* (Fig. 6). Ca^{2+} influx via AtANN1 could form a positive feedback, causing Ca^{2+}-dependent activation of AtRBOHC (Takeda et al., 2008) to maintain *AtSOS1* stability. Secondary root growth involves superoxide anion production, possibly by NADPH oxidases (Roach and Kranner, 2011). The involvement of these enzymes

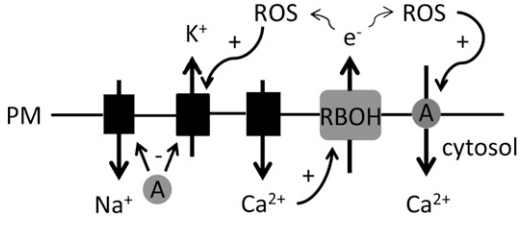

Figure 6. Schematic summary of possible events at the epidermal plasma membrane (PM) under salinity exposure. AtANN1 (A) is a negative regulator of Na^+ influx and K^+ efflux during salinity exposure, by unknown mechanism. AtANN1 is depicted as cytosolic but could be acting as a membrane integral or peripheral protein. K^+ efflux could be mediated by the $OH^{\bullet}$-activated GORK (Demidchik et al., 2010). NaCl or osmotic effect causes elevation of $[Ca^{2+}]_{cyt}$ by unknown mechanism; the participation of plasma membrane Ca^{2+}-permeable channels is shown. Elevation of $[Ca^{2+}]_{cyt}$ results in stimulation of NADPH oxidase (RBOH) activity (Takeda et al., 2008) and the resultant production of extracellular $OH^{\bullet}$ stimulates Ca^{2+} entry through AtANN1. At low external Ca^{2+}, AtRBOHC and AtANN1 are involved in *AtSOS1* stabilization (not shown).

may help explain why the *Atann1* mutant was compromised in its ability to generate secondary roots under salinity stress. As an ROS-activated Ca^{2+} transport pathway, AtANN1 is expected to lie downstream of NADPH oxidases. The impaired up-regulation of *AtSOS1* in the *Atann1* mutant may have contributed to impaired secondary root formation (Huh et al., 2002) when external Ca^{2+} was 1.5 mM. Although AtANN1 accounted for the high Ca^{2+}-dependent component of the NaCl-induced $[Ca^{2+}]_{cyt}$ response of epidermal protoplasts, secondary root formation by the *Atann1* mutant was not significantly lower than that of the wild type at high external Ca^{2+}. The pathway from AtANN1-mediated and -independent $[Ca^{2+}]_{cyt}$ increase to secondary root production now needs to be explored in greater detail and would be aided by single cell type studies (Kiegle et al., 2000; Dinneny et al., 2008).

Annexin up-regulation in salt-stressed crops such as chickpea (*Cicer arietinum*) and tomato (*Solanum lycopersicum*) has now been recorded (Manaa et al., 2011; Molina et al., 2011), pointing to positive roles in adaptation. Previously, AtANN1 was found to be important for drought tolerance (Konopka-Postupolska et al., 2009; Huh et al., 2010) and germination under salinity stress (Lee et al., 2004). This study has revealed AtANN1 to be a significant component of $[Ca^{2+}]_{cyt}$ signaling and adaptive root growth under salinity stress. The impaired ability of *Atann1* to form secondary roots under osmotic stress may help explain its drought sensitivity. In addition to mediating $[Ca^{2+}]_{cyt}$ signals, AtANN1 inhibits root Na^+ influx and K^+ efflux, pointing to annexins as tools to identify the underlying proteins in those critical transport routes and as future target proteins in their own right for consideration in the generation of crops with greater resilience to salinity stress.

CONCLUSION

Salinity-induced $[Ca^{2+}]_{cyt}$ increase in Arabidopsis roots requires AtANN1, especially for the component generated by oxidation. Results to date suggest that AtANN1 is acting directly as a Ca^{2+} transport route in the epidermal plasma membrane. How AtANN1 forms this pathway requires further examination. The *Atann1* mutant could be a useful tool in both the identification of Na^+ influx pathways and the elucidation of processes governing secondary root formation in adaptive growth.

MATERIALS AND METHODS

Plant Material and Growth Analysis

Arabidopsis (*Arabidopsis thaliana* ecotype Columbia), its *Atann1* homozygous transfer DNA loss-of-function mutant (single transfer DNA insert in the third exon of *At1g35720*; GenBank accession no. AF083913), the 35S-complemented mutant, and *Atann1* constitutively expressing cytosolic apoaequorin (35S promoter) were as described previously (Lee et al., 2004; Laohavisit et al., 2012). Plants were grown vertically on one-half-strength Murashige and Skoog medium with 1% (w/v) Suc and 0.8% (w/v) bactogar, pH 5.7. After a 2-d stratification, growth was at 25°C in a 16-h day at 100 μmol m^{-2} s^{-1} irradiance. In experiments on secondary roots, seedlings were transferred from control plates at 3 d to split medium plates in which the top 4 cm of medium was always control and the remainder was control or test. The hypocotyls bridged the interface between the two media so that the cotyledons were not exposed to the lower medium. D-Sorbitol (ultrapure) was used to generate equivalent osmolarity to NaCl tests, determined with a vapor pressure osmometer. Secondary roots were counted after 9 d and scanned at 300 dots per inch.

Flux Analysis

Net fluxes were measured from root epidermis of 6-d-old plants, using Na^+- and K^+-selective extracellular vibrating microelectrodes as described previously but with a 4-*tert*-butylcalix[4]arene-tetra acetic acid tetraethyl ester sensor for Na^+ (Shabala et al., 2006; Jayakannan et al., 2011). Measurements were taken from developmentally equivalent mature epidermis, 2 to 3 mm from the apex of immobilized root apical segments (8–10 mm). Analysis was as described previously (Shabala et al., 2006).

$[Ca^{2+}]_{cyt}$ Determination

Excised roots from 6- to 7-d-old seedlings were incubated in coelentrazine solution (10 μM coelentrazine [Lux Biotechnology], 10 mM $CaCl_2$, 0.1 mM KCl, and 2 mM Tris/MES, pH 5.8) for 4 h in the dark. Single roots (washed with coelentrazine-free buffer) were placed into wells of a white 96-well plate (Greiner Bio-One) with 100 μL buffer and recovered in darkness for 30 min. Root epidermal protoplasts were prepared for luminometry, and luminescence was recorded in a plate reader luminometer as described previously (Laohavisit et al., 2012). Occasionally, resting $[Ca^{2+}]_{cyt}$ was higher in the mutant than the wild type. Calibration to convert luminescent values to $[Ca^{2+}]_{cyt}$ was performed as described by Knight et al. (1997).

Planar Lipid Bilayers and Patch Clamp Electrophysiology

AtANN1 was expressed in *Saccharomyces cerevisiae*, purified by lipid affinity, and verified by immunoblotting as described previously (Laohavisit et al., 2012). Experiments were performed with protein from three separate purifications. Planar lipid bilayers were formed from 25 mg mL^{-1} (1-palmitoyl 2-oleoyl phosphatidylethanolamine, cholesterol, and 1-palmitoyl 2-oleoyl phosphatidyl-Ser in a 5:3:2 ratio, respectively, at room temperature [20°C–24°C] as described by Laohavisit et al. [2012]). Annexin (3 μg) protein was added to the cis chamber. The bilayer was held at –150 mV (cis negative) to aid insertion. $OH^{\bullet}$ were generated in the trans by 1 mM $CuCl_2$ and ascorbate (Laohavisit et al., 2012). $GdCl_3$ was also added to trans. For permeability estimates, the K^+-to-Cl^- permeability ratio of 53 was used, determined previously under identical recording conditions to those used here (Laohavisit et al., 2012). Patch clamp recordings on root epidermal protoplasts were as described by Laohavisit et al. (2012). Standard patch clamp procedures were applied (Véry and Davies, 2000).

Transcript Analysis

Salinity stress treatment and harvest were adapted from Dinneny et al. (2008). In each trial, a total of 35 to 40 7-d seedlings grown on solid control medium (1.5 mM Ca^{2+}) were transferred to untreated plates or plates containing 150 mM NaCl or 275 mM D-sorbitol for 24 h. Total RNA was extracted from excised roots using RNeasy Plant Mini Kit (Qiagen) according to manufacturer's protocol with a DNase digestion step (Qiagen). Prior to reverse transcription, RNA integrity was assessed on a 1% (w/v) agarose MOPS gel. RNA (500 ng) was reverse transcribed with QuantiTect Reverse Transcription Kit (Qiagen) according to manufacturer's instructions. Primers were as follows: *AtSOS1* (At2G01980), 5′-3′ CGGAAATTCACATATCAGCAAGG and 3′-5′ GAAGAAGGCGTAGAACAAATTGG; *AtRD29A* (At5G52310) 5′-3′ AACCACCACTCAACACACAC and 3′-5′ TCTTAGCTCTAGCCTTTACTTTCC; *AtDREB2A* (At5G05410) 5′-3′ TCGAGGTAGCAGGCTTTGGCT and 3′-5′ TCAGACGCATCAGACCGAGGGA; and *AtDREB2B* (At3G11020) 5′-3′ TCTTGTGGAACCAGGCCGGACA and 3′-5′ TGGCCCCAATACTGCTGCTCAA. Control primers were from the geNorm Arabidopsis reference gene kit (Primer Design; http://www.primerdesign.co.uk). This contains primer pairs for six endogenous control genes. All six primer pairs were tested on

complementary DNA from each treatment/genotype, encompassing a selection from each of the three biological replicates. Expression values were calculated from the cycle threshold (Ct) values as described in the geNorm handbook and put through the geNorm software. This determined how many internal controls were required for accurate normalization (in this case, two) and which primer pairs were the most stable across the treatments.

Specificity of primers was validated by sequencing amplicon and melt curve analysis. Quantitative PCR was performed with a Rotor-Gene 3000 thermocycler using Rotor-Gene SYBR Green PCR Kit (Qiagen; two technical replicates per reaction) following manufacturer's guidelines with 6 ng complementary DNA and 0.50 μM final primer concentration. Absence of genomic DNA in RNA was confirmed with a no reverse transcription control. Six endogenous control primers from the Arabidopsis geNorm kit were tested for stability across all treatment groups (control, NaCl, and sorbitol) using geNorm software (Vandesompele et al., 2002) according to manufacturer's guidelines. The mean reaction efficiencies (within ± 5% of the median efficiency) of each primer pair were quantified using LinReg PCR software (Ramakers et al., 2003). Quantification of targets was calculated based on the Pfaffl model (Pfaffl, 2001): reaction efficiency $(RE)^{-Ct\ target}$ normalized by the geometric mean of $RE^{-Ct\ endogenous\ controls}$. All data are from three independent trials. Significance was tested by two-way ANOVA (genotype and treatment as the two factors) with Holm-Sidak post hoc analyses.

Sequence data from this article can be found in the GenBank/EMBL data libraries under accession numbers AF083913, *Atann1,* At1g35720; AB007791, *AtDREB2A,* At5G05410; AB016571, *AtDREB2B,* At3g11020; AB056455; *AtRD29A,* At5g52310; AF256224, *AtSOS1,* and At2g01980.

Supplemental Data

The following materials are available in the online version of this article.

Supplemental Figure S1. $[Ca^{2+}]_{cyt}$ responses of root epidermal protoplasts.

Supplemental Figure S2. $[Ca^{2+}]_{cyt}$ elevation is impaired in single, excised *Atann1* roots.

Supplemental Figure S3. AtANN1 forms a cation conductance in artificial planar lipid bilayers.

Supplemental Figure S4. Root adaptation to salinity requires AtANN1.

Received March 15, 2013; accepted July 23, 2013; published July 25, 2013.

LITERATURE CITED

Ali R, Ma W, Lemtiri-Chlieh F, Tsaltas D, Leng Q, von Bodman S, Berkowitz GA (2007) Death don't have no mercy and neither does calcium: *Arabidopsis* CYCLIC NUCLEOTIDE GATED CHANNEL2 and innate immunity. Plant Cell **19:** 1081–1095

Chung JS, Zhu JK, Bressan RA, Hasegawa PM, Shi HZ (2008) Reactive oxygen species mediate Na^+-induced SOS1 mRNA stability in *Arabidopsis*. Plant J **53:** 554–565

Demidchik V, Cuin TA, Svistunenko D, Smith SJ, Miller AJ, Shabala S, Sokolik A, Yurin V (2010) Arabidopsis root K^+-efflux conductance activated by hydroxyl radicals: single-channel properties, genetic basis and involvement in stress-induced cell death. J Cell Sci **123:** 1468–1479

Demidchik V, Shang Z, Shin R, Thompson E, Rubio L, Laohavisit A, Mortimer JC, Chivasa S, Slabas AR, Glover BJ, et al (2009) Plant extracellular ATP signalling by plasma membrane NADPH oxidase and Ca^{2+} channels. Plant J **58:** 903–913

Demidchik V, Tester M (2002) Sodium fluxes through nonselective cation channels in the plasma membrane of protoplasts from Arabidopsis roots. Plant Physiol **128:** 379–387

Dinneny JR, Long TA, Wang JY, Jung JW, Mace D, Pointer S, Barron C, Brady SM, Schiefelbein J, Benfey PN (2008) Cell identity mediates the response of *Arabidopsis* roots to abiotic stress. Science **320:** 942–945

Dodd AN, Jakobsen MK, Baker AJ, Telzerow A, Hou SW, Laplaze L, Barrot L, Poethig RS, Haseloff JP, Webb AAR (2006) Time of day modulates low-temperature Ca signals in Arabidopsis. Plant J **48:** 962–973

Dodd AN, Kudla J, Sanders D (2010) The language of calcium signaling. Annu Rev Plant Biol **61:** 593–620

Foreman J, Demidchik V, Bothwell JHF, Mylona P, Miedema H, Torres MA, Linstead P, Costa S, Brownlee C, Jones JDG, et al (2003) Reactive oxygen species produced by NADPH oxidase regulate plant cell growth. Nature **422:** 442–446

Gobert A, Park G, Amtmann A, Sanders D, Maathuis FJM (2006) *Arabidopsis thaliana* cyclic nucleotide gated channel 3 forms a non-selective ion transporter involved in germination and cation transport. J Exp Bot **57:** 791–800

Gorecka KM, Thouverey C, Buchet R, Pikula S (2007) Potential role of annexin AnnAt1 from *Arabidopsis thaliana* in pH-mediated cellular response to environmental stimuli. Plant Cell Physiol **48:** 792–803

Guo KM, Babourina O, Christopher DA, Borsics T, Rengel Z (2008) The cyclic nucleotide-gated channel, AtCNGC10, influences salt tolerance in Arabidopsis. Physiol Plant **134:** 499–507

Huh GH, Damsz B, Matsumoto TK, Reddy MP, Rus AM, Ibeas JI, Narasimhan ML, Bressan RA, Hasegawa PM (2002) Salt causes ion disequilibrium-induced programmed cell death in yeast and plants. Plant J **29:** 649–659

Huh SM, Noh EK, Kim HG, Jeon BW, Bae K, Hu HC, Kwak JM, Park OK (2010) Arabidopsis annexins AnnAt1 and AnnAt4 interact with each other and regulate drought and salt stress responses. Plant Cell Physiol **51:** 1499–1514

Jayakannan M, Babourina O, Rengel Z (2011) Improved measurements of Na^+ fluxes in plants using calixarene-based microelectrodes. J Plant Physiol **168:** 1045–1051

Jiang CF, Belfield EJ, Mithani A, Visscher A, Ragoussis J, Mott R, Smith JAC, Harberd NP (2012) ROS-mediated vascular homeostatic control of root-to-shoot soil Na delivery in Arabidopsis. EMBO J **31:** 4359–4370

Kaye Y, Golani Y, Singer Y, Leshem Y, Cohen G, Ercetin M, Gillaspy G, Levine A (2011) Inositol polyphosphate 5-phosphatase7 regulates the production of reactive oxygen species and salt tolerance in Arabidopsis. Plant Physiol **157:** 229–241

Kiegle E, Moore CA, Haseloff J, Tester M, Knight MR (2000) Cell-type specific calcium responses to drought, NaCl and cold in *Arabidopsis* root: a role for endodermis and pericycle in stress signal transduction. Plant J **23:** 267–278

Knight H, Trewavas AJ, Knight MR (1997) Calcium signalling in *Arabidopsis thaliana* responding to drought and salinity. Plant J **12:** 1067–1078

Konopka-Postupolska D, Clark G, Goch G, Debski J, Floras K, Cantero A, Fijolek B, Roux S, Hennig J (2009) The role of annexin 1 in drought stress in Arabidopsis. Plant Physiol **150:** 1394–1410

Kronzucker HJ, Britto DT (2011) Sodium transport in plants: a critical review. New Phytol **189:** 54–81

Kung C-CS, Huang W-N, Huang Y-C, Yeh K-C (2006) Proteomic survey of copper-binding proteins in *Arabidopsis* roots by immobilized metal affinity chromatography and mass spectrometry. Proteomics **6:** 2746–2758

Laohavisit A, Brown AT, Cicuta P, Davies JM (2010) Annexins: components of the calcium and reactive oxygen signaling network. Plant Physiol **152:** 1824–1829

Laohavisit A, Davies JM (2011) Annexins. New Phytol **189:** 40–53

Laohavisit A, Mortimer JC, Demidchik V, Coxon KM, Stancombe MA, Macpherson N, Brownlee C, Hofmann A, Webb AAR, Miedema H, et al (2009) *Zea mays* annexins modulate cytosolic free Ca^{2+}, form a Ca^{2+}-permeable conductance and have peroxidase activity. Plant Cell **21:** 479–493

Laohavisit A, Shang ZL, Rubio L, Cuin TA, Véry AA, Wang AH, Mortimer JC, Macpherson N, Coxon KM, Battey NH, et al (2012) *Arabidopsis* annexin1 mediates the radical-activated plasma membrane Ca^{2+}- and K^+-permeable conductance in root cells. Plant Cell **24:** 1522–1533

Lee S, Lee EJ, Yang EJ, Lee JE, Park AR, Song WH, Park OK (2004) Proteomic identification of annexins, calcium-dependent membrane binding proteins that mediate osmotic stress and abscisic acid signal transduction in *Arabidopsis*. Plant Cell **16:** 1378–1391

Liu SG, Zhu DZ, Chen GH, Gao XQ, Zhang XS (2012) Disrupted actin dynamics trigger an increment in the reactive oxygen species levels in the *Arabidopsis* root under salt stress. Plant Cell Rep **31:** 1219–1226

Lynch J, Polito VS, Läuchli A (1989) Salinity stress increases cytoplasmic ca activity in maize root protoplasts. Plant Physiol **90:** 1271–1274

Ma LY, Zhang H, Sun LR, Jiao YH, Zhang GZ, Miao C, Hao FS (2012) NADPH oxidase AtrbohD and AtrbohF function in ROS-dependent

regulation of Na^+/K^+ homeostasis in Arabidopsis under salt stress. J Expt Bot **63:** 305–317

Manaa A, Ben Ahmed H, Valot B, Bouchet JP, Aschi-Smiti S, Causse M, Faurobert M (2011) Salt and genotype impact on plant physiology and root proteome variations in tomato. J Exp Bot **62:** 2797–2813

Molina C, Zaman-Allah M, Khan F, Fatnassi N, Horres R, Rotter B, Steinhauer D, Amenc L, Drevon JJ, Winter P, et al (2011) The salt-responsive transcriptome of chickpea roots and nodules via deep-SuperSAGE. BMC Plant Biol **11:** 31

Munns R, Tester M (2008) Mechanisms of salinity tolerance. Annu Rev Plant Biol **59:** 651–681

Nakashima K, Ito Y, Yamaguchi-Shinozaki K (2009) Transcriptional regulatory networks in response to abiotic stresses in Arabidopsis and grasses. Plant Physiol **149:** 88–95

Pfaffl MW (2001) A new mathematical model for relative quantification in real-time RT-PCR. Nucleic Acids Res **29:** e45

Ramakers C, Ruijter JM, Deprez RHL, Moorman AFM (2003) Assumption-free analysis of quantitative real-time polymerase chain reaction (PCR) data. Neurosci Lett **339:** 62–66

Roach T, Kranner I (2011) Extracellular superoxide production associated with secondary root growth following desiccation of *Pisum sativum* seedlings. J Plant Physiol **168:** 1870–1873

Shabala S, Demidchik V, Shabala L, Cuin TA, Smith SJ, Miller AJ, Davies JM, Newman IA (2006) Extracellular Ca^{2+} ameliorates NaCl-induced K^+ loss from Arabidopsis root and leaf cells by controlling plasma membrane K^+ -permeable channels. Plant Physiol **141:** 1653–1665

Shi H, Ishitani M, Kim C, Zhu JK (2000) The *Arabidopsis thaliana* salt tolerance gene *SOS1* encodes a putative Na^+/H^+ antiporter. Proc Natl Acad Sci USA **97:** 6896–6901

Takeda S, Gapper C, Kaya H, Bell E, Kuchitsu K, Dolan L (2008) Local positive feedback regulation determines cell shape in root hair cells. Science **319:** 1241–1244

Tracy FE, Gilliham M, Dodd AN, Webb AAR, Tester M (2008) NaCl-induced changes in cytosolic free Ca^{2+} in *Arabidopsis thaliana* are heterogeneous and modified by external ionic composition. Plant Cell Environ **31:** 1063–1073

Vandesompele J, De Preter K, Pattyn F, Poppe B, Van Roy N, De Paepe A, Speleman F (2002) Accurate normalization of real-time quantitative RT-PCR data by geometric averaging of multiple internal control genes. Genome Biology **3:** research0034.1–research0034.11

Véry A-A, Davies JM (2000) Hyperpolarization-activated calcium channels at the tip of *Arabidopsis* root hairs. Proc Natl Acad Sci USA **97:** 9801–9806

Vincill ED, Bieck AM, Spalding EP (2012) Ca^{2+} conduction by an amino acid-gated ion channel related to glutamate receptors. Plant Physiol **159:** 40–46

Xie YJ, Xu S, Han B, Wu MZ, Yuan XX, Han Y, Gu QA, Xu DK, Yang Q, Shen WB (2011) Evidence of *Arabidopsis* salt acclimation induced by up-regulation of *HY1* and the regulatory role of RbohD-derived reactive oxygen species synthesis. Plant J **66:** 280–292

Yang YL, Xu SJ, An LZ, Chen NL (2007) NADPH oxidase-dependent hydrogen peroxide production, induced by salinity stress, may be involved in the regulation of total calcium in roots of wheat. J Plant Physiol **164:** 1429–1435